Threshold photodetachment zero-electron kinetic energy spectroscopy of Si− 3

Caroline C. Arnold and Daniel M. Neumark

Citation: The Journal of Chemical Physics **100**, 1797 (1994); doi: 10.1063/1.466532
View online: http://dx.doi.org/10.1063/1.466532
View Table of Contents: http://scitation.aip.org/content/aip/journal/jcp/100/3?ver=pdfcov
Published by the AIP Publishing

Threshold photodetachment zero-electron kinetic energy spectroscopy of Si_3^-

Caroline C. Arnold and Daniel M. Neumark[a)]
University of California, Berkeley, California 94720 and Chemical Sciences Division, Lawrence Berkeley Laboratory, Berkeley, California 94720

(Received 27 August 1993; accepted 13 October 1993)

The threshold photodetachment zero-electron kinetic energy (ZEKE) spectrum of Si_3^- is presented and discussed. The spectrum shows well-resolved vibrational structure. A comparison with several *ab initio* calculations shows that the spectrum is due to transitions to the $^3A_2'$ (D_{3h}) state of Si_3. The symmetric stretch and degenerate e' frequencies for the Si_3 $^3A_2'$ state are determined to be 501 ± 10 and 337 ± 10 cm^{-1}, respectively. Additional structure observed in the spectrum suggests that the negative ion is a fluxional, Jahn–Teller distorted species. The ZEKE spectrum shows no evidence for transitions to the $^1A_1$ state of the neutral, which is predicted to lie very close to the $^3A_2'$ state. A comparison of the ZEKE and previously obtained photoelectron spectrum of Si_3^- suggests that these two states are close in energy, but that transitions to the singlet state are very weak in the ZEKE spectrum.

I. INTRODUCTION

The study of small silicon clusters has been motivated by their importance in astrophysics[1] and chemical vapor deposition processes.[2] The desire to characterize these species experimentally has been further fueled by a series of *ab initio* studies that have predicted interesting electronic properties and structural trends as a function of cluster size.[3] However, other than for the dimer,[4,5] experimental work on these elusive species is sparse; thus far, vibrationally resolved spectra have been obtained only for Si_3 and Si_4,[6–8] and no rotationally resolved spectra have been observed for any species larger than the dimer. In our laboratory, we are focusing on probing the electronic and vibrational structure of these clusters by performing high resolution photodetachment spectroscopy experiments. This paper discusses the results of such a study performed on Si_3.

Silicon trimer has been the object of considerable theoretical efforts, starting with the work by Grev and Schaefer[9] and by Raghavachari[10] in 1985. The results of their calculations for an extensive set of molecular structures indicated that, in contrast to the well-known linear structure of C_3,[11] Si_3 is strongly bent, with two close lying electronic states—the $^1A_1$ (C_{2v}) and $^3A_2'$ (D_{3h}) states. Both calculations predict the singlet C_{2v} structure to be the ground state, but the calculated spacing between the two states is less than 1 kcal/mol. More recent calculations have yielded similar results.[12–15] The negative ion of Si_3, while less studied, is also interesting from a theoretical standpoint. Rohlfing and Raghavachari[16,17] reported a $^2A_1$ (C_{2v} geometry) ground state which results from Jahn–Teller distortion of a $^2E'$ configuration, with the corresponding $^2B_2$ saddle point lying only 160 cm^{-1} higher in energy. Raghavachari[10,16,17] has calculated vibrational frequencies for the anion as well as the low-lying neutral states, and frequencies for the neutral states have also been calculated by Dixon and Gole[12] and Depristo.[14]

The experimental work to date on Si_3/Si_3^- has not been of sufficient quality to test the *ab initio* predictions concerning electronic and vibrational structure. The negative ion photoelectron spectrum (PES) of Si_3^- obtained by Smalley and co-workers[18] revealed several electronic bands, but the resolution was insufficient to make any assignments. In the vibrationally resolved PES of Si_3^- obtained by our group,[6] we observed that the band associated with the lowest Si_3 electronic state exhibited an extended vibrational progression with a characteristic frequency of 360 ± 40 cm^{-1}; in poor agreement with the calculated frequencies of the purported ground $^1A_1$ state. However, this progression was congested and poorly resolved, and a better quality spectrum was clearly needed for comparison with the *ab initio* work. A similar frequency was observed in emission spectra obtained by Gole and co-workers[7] and attributed to Si_3.

In this paper, the substantially higher resolution threshold photodetachment (zero electron kinetic energy, or ZEKE) spectrum of Si_3^- is presented. As with the ZEKE spectra we obtained for Si_2^- and Si_4^-,[5,8] more detailed information regarding both the Si_3 anion and neutral electronic states is extracted from the spectrum presented below than could be determined from the PES. The spectrum, which could be obtained over only a small part of the energy range probed by the PES, shows well-resolved transitions between what appear to be the ground electronic states of the anion and neutral trimer. This spectral structure, however, is still not reconcilable with the predicted $^2A_1$ anion and $^1A_1$ neutral ground state frequencies.[10,12,14,17] Instead, it appears that the band is due to transitions to the neutral $^3A_2'$ (D_{3h}) state which, as mentioned above, is predicted to be nearly degenerate with, but slightly higher in energy than the calculated neutral ground $^1A_1$ state. The ZEKE spectrum also exhibits additional structure not resolved in the PES. In order to satisfactorily assign this structure, it is necessary to treat the

[a)]NSF Presidential Young Investigator and Camille and Henry Dreyfus Teacher–Scholar.

 0021-9606/94/100(3)/1797/8/$6.00

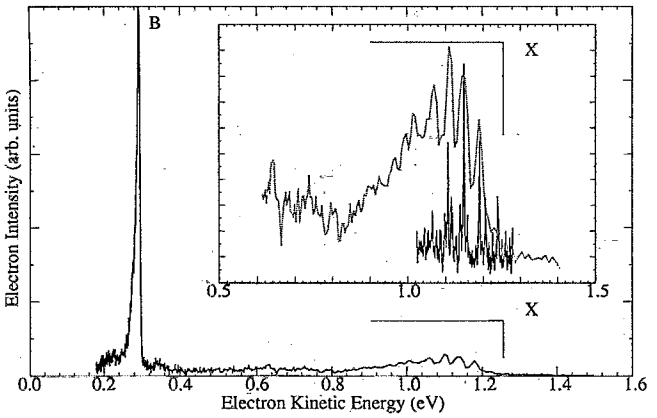

FIG. 1. Photoelectron spectrum of Si_3^- obtained using 3.493 eV photon energy with the threshold photodetachment (ZEKE) spectrum superimposed on the inset.

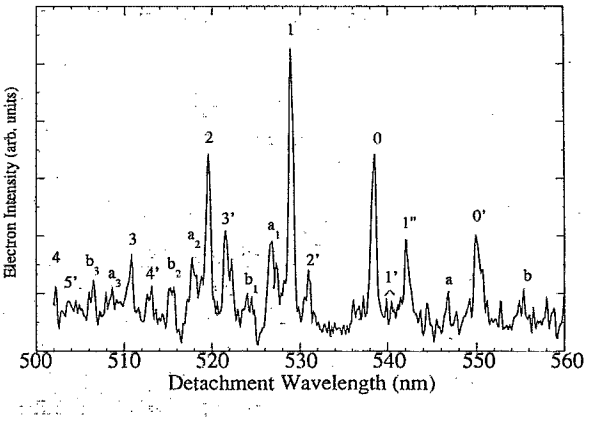

FIG. 2. Threshold photodetachment spectrum of Si_3^-.

anion as a fluxional, Jahn–Teller distorted species rather than as a rigid molecule.

II. EXPERIMENT

The threshold photodetachment spectrometer used in this study is described in detail elsewhere,[19] but the basic operation is as follows: A beam of cold silicon cluster anions is generated in a laser vaporization/pulsed molecular beam source and is mass selected using time of flight. The cluster of interest is then photodetached using an excimer-pumped dye laser operated at 20 Hz. The electrons detached with nearly zero kinetic energy (ZEKE) are collected as a function of photon wavelength. The selective detection of ZEKE electrons, based on the method developed by Müller-Dethlefs *et al.*,[20] gives an energy resolution as good as 3 cm^{-1}. However, because of the small photodetachment cross section of Si_3^-, some resolution was sacrificed for increased signal; the resolution for the spectrum presented below is estimated to be 10–15 cm^{-1}. The signal was averaged for 1500 shots at each wavelength and normalized to both laser power and ion current. The two dyes used to obtain the spectrum were coumarin 540 and coumarin 503.

III. RESULTS

Figure 1 shows the PES of Si_3^- previously obtained with a detachment wavelength of 355 nm (3.493 eV).[6] Band X represents transitions to the lowest electronic state(s) of Si_3, while band B is a transition to a more highly excited state. The inset shows band X on an expanded y axis (dotted line) with the newly obtained ZEKE spectrum superimposed onto the PES energy scale. We observed a ZEKE spectrum for this band only. The data collection was considerably more time consuming than in our recent study of Si_4^- (Ref. 8); the photodetachment cross section near threshold was much smaller for Si_3^- than for Si_4^-, and the trimer ions were more difficult to produce. Figure 2 shows the ZEKE spectrum of band X on an expanded scale showing the detachment wavelength. The spectrum is dominated by a 337 cm^{-1} progression formed by the 18–20 cm^{-1} wide [full width at half-maximum (FWHM)] peaks labeled 0, 1, 2, 3, and 4. Peak 0′ is not a member of this progression; it lies 385 cm^{-1} to the lower photon energy of peak 0, which appears to be the origin of the main progression. This 337 cm^{-1} progression is congested with lower intensity peaks, sometimes hardly discernible from the noise, spaced fairly regularly about the progression members. For example, peaks 1′, 2′,...,5′ are found ~80 cm^{-1} to the red of peaks 0,...,4, respectively. Peaks a_1, a_2, and a_3 are found ~80 cm^{-1} to the blue and peaks b_1, b_2, and b_3 are found roughly 160 cm^{-1} to the blue of peaks 1, 2, and 3, respectively. There are no corresponding peaks a_0 or b_0 to the blue of peak 0. Additional structure occurs to the red of the origin. The fairly intense peak 1″ is found 128 cm^{-1} to the red of peak 0, and two very low intensity peaks, labeled a and b, occur at ~280 and 565 cm^{-1} to the red of peak 0, respectively. The peak labels, positions, and relative energies are summarized in Table I.

IV. ANALYSIS AND DISCUSSION

A. Assignment of electronic and vibrational structure

The high level calculations [QCISD(T)/6-31G*] performed by Rohlfing and Raghavachari[17] have predicted both the anion and neutral ground states to be isosceles (C_{2v}) triangles, where the Si–Si–Si bond angle (θ) is 65.2° for the $^2A_1$ anion ground state and 79.6° for the $^1A_1$ neutral ground state. The neutral structure is the result of Jahn–Teller distortion of the $^1E'$ (D_{3h}) state, which is formed by the

$$(1a_1')^2(1e')^4(2a_1')^2(1a_2'')^2(2e')^2 \qquad \text{(configuration 1)}$$

configuration. This distortion to C_{2v} geometry, which causes the degenerate e' orbitals to split into a_1 and b_2 orbitals, results in the $^1A_1$ state with the

$$(a_1)^2(b_2)^2(a_1)^2(a_1)^2(b_1)^2(b_2)^2 \qquad \text{(configuration 2)}$$

configuration and a more acute $^1B_2$ state. The $^1A_1$ state is calculated to be much lower in energy than the $^1B_2$ state due to second order Jahn–Teller stabilization effects. The

TABLE I. Peak positions, relative energies, and proposed assignments for the Si_3^- ZEKE spectrum. The assignments, shown as $^3A_2'$ (v_1, $v_{e'}$, m) $\leftarrow$ $^2A_1$ (v_1, v_2, j), are based on quadratic Jahn–Teller spectral simulation (see the text). Uncertainties in peak positions are given in parentheses. When more than one transition contributes to a peak, the transitions are listed in order of decreasing contribution.

Peak	Position (nm)	Relative energy (cm^{-1})	Possible transition in order of descending intensity
b	555.55	−565(15)	(0,0,0) ← (1,0,1/2)
0′	550.05	−385(12)	(0,0,0) ← (0,1,1/2)
a	546.95	−282(10)	(0,0,0) ← (0,0,5/2)
1″	542.40	−128(10)	?
1′	540.55	−62(20)	(1,0,0) ← (1,0,1/2)
0	**538.65**	**0(7)**	**origin**
2′	531.20	260(10)	(0,1,1) ← (0,0,3/2±), (1,1,1) ← (1,0,1/2) (0,2,0) ← (0,1,1/2)
1	**529.05**	**337(10)**	**(0,1,0) ← (0,0,1/2)**
a_1	526.85	416(15)	(0,2,2) ← (0,0,5/2)
b_1	524.40	504(15)	(1,0,0) ← (0,0,1/2), (0,3,1) ← (0,1,3/2)
3′	521.95	594(15)	(0,2,2) ← (0,0,3/2+), (0,3,3) ← (0,0,7/2) (0,3,1) ← (0,1,1/2), (0,2,0) ← (1,0,1/2)
2	**519.74**	**675(10)**	**(0,2,0) ← (0,0,1/2)**
a_2	517.79	748(15)	(0,3,2) ← (0,0,5/2)
b_2	515.34	840(15)	(1,1,1) ← (0,0,1/2), (0,4,2) ← (0,1,3/2)
4′	513.0	928(20)	(0,3,1) ← (0,0,3/2), (0,4,4) ← (0,0,7/2) (0,4,0) ← (0,1,1/2), (1,3,1) ← (1,0,1/2)
3	**510.94**	**1007(10)**	**(0,3,0) ← (0,0,1/2)**
a_3	508.39	1106(20)	(0,4,2) ← (0,0,5/2)
b_3	506.64	1173(15)	(1,2,0) ← (0,0,1/2), (0,5,1) ← (0,1,3/2)
5′	504.30	1264(30)	(0,4,1) ← (0,0,3/2), (0,5,3) ← (0,0,7/2) (0,5,1) ← (0,1,1/2), (1,4,0) ← (1,0,1/2)
4	**502.39**	**1340(10)**	**(0,4,0) ← (0,0,1/2)**

undistorted (D_{3h}) $^3A_2'$ state, which has been calculated to be nearly degenerate with the $^1A_1$ state,[9,10,17] has the orbital occupancy of configuration (1) with parallel spins in the $2e'$ orbitals.

The anion ground state is obtained by adding an electron to the $2e'$ orbital of configuration (1), resulting in a $^2E'$ state. This state is also subject to Jahn–Teller distortion to the previously mentioned $^2A_1$ state with the orbital occupation

$$\ldots(a_1)^2(b_1)^2(b_2)^2(a_1)^1 \qquad \text{(configuration 3)}$$

and a $^2B_2$ state with $\theta \approx 57°$. At the Hartree–Fock level, $^2B_2$ is the ground state and $^2A_1$ is the saddle point on the typical J–T distorted potential, but upon including electron correlation effects, these are reversed and $^2A_1$ becomes more stable at the QCISD(T) level by ~ 160 cm^{-1}.[16,17] This energy difference corresponds to the pseudorotation barrier.

The 337 cm^{-1} progression seen both in the PES (Fig. 1) and, more definitively, in the ZEKE spectrum appears to be due to transitions between the ground anion state and vibrational levels in the ground neutral state. Because of the large bond angle difference between the $^2A_1$ anion and the $^1A_1$ neutral, the symmetric bend mode (v_2) should be the most active in the spectrum. However, this mode is consistently calculated to be approximately 150–170 cm^{-1},[9,10,14,17] which is approximately half the observed frequency. The symmetric stretch mode (v_1), which could also be active in the spectrum, has a calculated frequency of 551 cm^{-1}, much higher than the observed frequency. This suggests that the band in our spectrum does not represent transitions to the $^1A_1$ neutral state.

Alternatively, the calculated e' frequency of the $^3A_2'$ (D_{3h}) state is in better agreement with the spacing in the observed progression. Raghavachari[17] and Schaefer[9] calculated a frequency of approximately 285 cm^{-1} for the e' mode using the QCISD(T) and self-consistent field (SCF) methods, respectively. Density functional studies on the D_{3h} structure performed by Dixon and Gole,[12] Dupuis,[13] and DePristo[14] yielded values ~ 340 cm^{-1} for the e' frequency. Because the calculated e' frequency is in better agreement than either of the $^1A_1$ frequencies with the observed 337 cm^{-1} progression, we believe that the band in the ZEKE spectrum is due to the $^3A_2' + e^- \leftarrow {}^2A_1$ transition and that the 337 cm^{-1} progression can be assigned to transitions to levels in the v_2 (e') mode of the neutral; this was first suggested in Dixon's comparison of *ab initio* frequencies with the experimental photoelectron and emission spectra.[12] Although long progressions seen in photodetachment spectra are generally only in totally symmetric modes of the neutral, one component of the e' vibration transforms as the symmetric v_2 (a_1) bend mode of the C_{2v} an-

ion. Therefore, in the rigid molecule limit (the first situation that we will treat), transitions from the totally symmetric ground state of the anion to any quanta in the neutral mode are allowed. Hence we assign each peak n to 2_0^n transition.

Based on further comparison of the ZEKE spectrum with *ab initio* frequency calculations, we can assign peak b_1 to the 1_0^1 transition, yielding 501 ± 10 cm^{-1} for the neutral ν_1 frequency. This is in good agreement with all of the calculations for the symmetric stretch (ν_1) frequency of the $^3A_2'$ state, but the density functional studies again give the closest value, approximately 500 cm^{-1}. Peaks b_2,...,b_4 can then be assigned to $\nu_1+n\nu_2$ ($1_0^1 2_0^n$) combination bands.

The structure found to lower photon energy from the origin was found to depend on ion source conditions, suggesting that they are transitions from vibrationally excited levels of the anion (hot band transitions). The most intense hot bands are those labeled 0′ and 1″, with peaks b and a being less intense. Because the ν_2 mode is the most active in the spectrum, we can tentatively assign 0′ to the 2_1^0 transition. The position of peak 0′ with respect to the origin would give an anion frequency of 385 cm^{-1}, which is in poor agreement with the calculated value 297 cm^{-1}.[17] Peak b, found 565 cm^{-1} from the origin, can be assigned tentatively to the 1_1^0 transition, giving the anion ν_1 frequency in fairly good agreement with the 533 cm^{-1} calculated frequency.[17]

The remaining structure found to higher photon energy from the origin, such as peaks n' and a_n, also appears to be due to transitions from excited vibrational levels in the anion. Based on the ν_1 and ν_2 anion and neutral frequencies determined above, sequence bands originating from either the $\nu_2=1$ or $\nu_3=1$ anion levels should fall to the red of the corresponding 2_0^n transition, in the energetic vicinity of peaks n'. Peaks a_n, slightly to the blue of each 2_0^n transition, could then be sequence bands in the ν_3 mode, giving an anion frequency of less than 337 cm^{-1} for this mode.

Since we have determined that the neutral Si_3 state in the ZEKE spectrum has D_{3h} symmetry, we can attempt to extract information regarding the anion geometry most simply by assuming that the anion has a rigid, C_{2v} structure. With this assumption, we can treat the profile of the progression by performing spectral simulations within the Franck–Condon approximation, where we assume the vibrational wave functions of the anion and neutral are the products of three harmonic oscillators representing the three normal modes. The intensity of a transition between vibrational levels in the anion and neutral is therefore proportional to the Franck–Condon factors of the two levels. The neutral and anion frequencies are fixed by the above assignments; note that the neutral is treated as a C_{2v} species with $\nu_2=\nu_3=337$ cm^{-1} (where ν_3 in this instance corresponds to the component of the neutral degenerate mode that transforms as b_2 in C_{2v} geometry).

This "rigid anion" simulation is shown in the second panel of Fig. 3. The profile of the 337 cm^{-1} progression was well matched by assuming a normal mode displacement (from anion to neutral) of $\Delta Q_2=0.095$ Å amu$^{1/2}$,

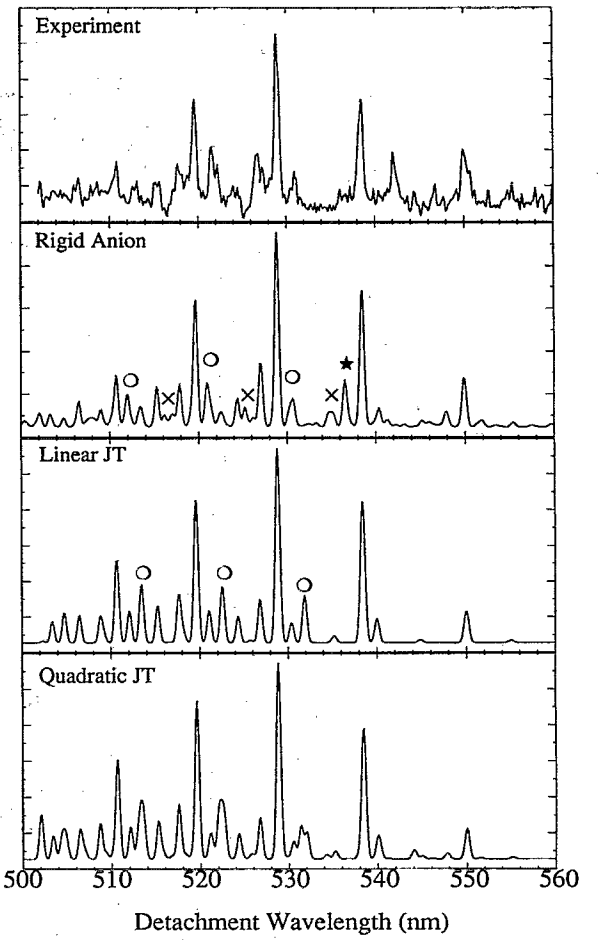

FIG. 3. Experimental spectrum and three simulations (see the text): rigid anion, linear Jahn–Teller (LJT), and quadratic Jahn–Teller (QJT). All three simulations assume 337 cm^{-1} (e') and 500 cm^{-1} (a_1) neutral frequencies. The rigid anion simulation assumes the following anion frequencies (and temperatures); $\nu_1=560$ cm^{-1} (500 K); $\nu_2=385$ cm^{-1} (450 K); $\nu_3=270$ cm^{-1} (350 K). LJT assumes 120 K for the 0,0,3/2 level, 250 K for the 0,0,5/2 level, 350 K for the 0,1,1/2 level (385 cm^{-1} above ground), 350 K for the 0,0,7/2 level, and 400 K for the (0,1,3/2), (1,0,1/2), and (1,0,3/2) levels. QJT assumes 150 K for the 0,0,3/2 levels (degeneracy broken), otherwise, temperatures are the same as LJT simulation.

given that the anion frequency for this mode is 385 cm^{-1}. The lower intensity b_n peaks (the $1_0^1 2_0^n$ transitions) were accounted for by assuming $\Delta Q_1=0.03$ Å amu$^{1/2}$. These two displacements compare well to the predicted displacements between the anion and neutral based on Raghavachari's geometry calculations and our own determination of the normal mode coordinates $\Delta Q_2=0.117$ Å amu$^{1/2}$ and $\Delta Q_1=0.03$ Å amu$^{1/2}$.

The intensities of all transitions originating from vibrationally excited levels in the anion are dependent on vibrational temperature. In general, the lower frequency modes tend to have lower temperatures than the higher frequency modes. This is not unusual since different modes are expected to cool with different efficiencies in a molecular beam. Temperatures for the various levels are included in the figure caption.

While the geometry changes between the anion and

neutral determined from this simple treatment are in good agreement with the calculated geometries, the rigid anion simulation exhibits several inadequacies in reproducing the positions and intensities of the sequence bands, namely, the a_n and n' peaks. First, the difference in frequencies between the anion and neutral symmetric bend produces sequence bands of the type 2_1^{n+1}, marked with circles on the simulation shown in Fig. 3. These occur approximately 50 cm^{-1} to the red of the main 2_0^n peaks. Also contributing to the intensity of these simulated peaks are $1_1^1 2_0^n$ sequence bands, which occur 65 cm^{-1} to the red of the 2_0^n peaks. This is in contrast to the actual position of peaks n', which are found 80 cm^{-1} to the red of the main peaks. This discrepancy is small but significant. Additionally, as mentioned above, peaks a_1, a_2, and a_3 can be proposed as $2_0^n 3_1^1$ transitions, which would yield an anion ν_3 frequency of approximately 270 cm^{-1} (the frequency used in the rigid anion simulation shown). However, this also produces a fairly intense sequence band to the blue of the origin, marked with a star, which is hardly present in the actual spectrum. There is also no structure in the experimental spectrum where the 3_2^2 sequence bands are predicted to lie (these are marked with an "x" on the Franck–Condon simulation). Finally, this analysis implies anion ν_2 and ν_3 frequencies of 385 and 270 cm^{-1}, respectively. This frequency ordering is unusual for a C_{2v} molecule with a bond angle greater than 60°, and is the reverse of the calculated ordering (ν_2=297 cm^{-1} and ν_3=370 cm^{-1}).[17] Taken together, all of these problems suggest that the analysis is partially flawed, and that it is naive to treat the anion as a simple, rigid C_{2v} molecule with uncoupled modes.

B. Inclusion of Jahn–Teller distortion in Si_3^-

Since the barrier to pseudorotation in Si_3^- is calculated to be only 160 cm^{-1}, an alternative approach to that outlined above is to analyze the ZEKE spectrum by treating the anion as fluxional, rather than as a rigid molecule. This situation arises in symmetric molecules having a set of spatially degenerate electronic states which are vibronically coupled by a degenerate vibration. The end result is a Jahn–Teller distortion of the molecule along the corresponding normal coordinate, removing the electronic degeneracy with the lowering of symmetry. In the case of Si_3^-, we have a species distorted from a symmetric D_{3h} equilibrium geometry because the e' degenerate vibration couples the two components of the $^2E'$ electronic state (see Sec. III A).

The $E\times e$ coupling problem can be approached most simply by assuming that the vibronic coupling term is linear with respect to the e' normal coordinate, i.e., no barrier to pseudorotation. In the basis of the two electronic states, and with the degenerate two-dimensional harmonic oscillator expressed in polar coordinates (ρ,ϕ), the vibrational energies and wave functions are determined from

$$\begin{pmatrix} H_0-E & k\rho e^{-i\phi} \\ k\rho e^{i\phi} & H_0-E \end{pmatrix}\begin{pmatrix}\chi_+ \\ \chi_-\end{pmatrix}=0, \tag{1}$$

where H_0 is the unperturbed Hamiltonian; k is a unitless parameter such that $\omega_2 k^2/2$ is the stabilization energy from the distortion; ω_2, in this instance, is the harmonic frequency of the e' mode in the undistorted molecule (often referred to as ω_0); and $\chi_\pm$ are the undistorted vibrational wave functions associated with the two electronic states. The implications of this have been studied extensively by Longuet-Higgens,[21] and Whetten,[22] e.g., and this treatment has been applied to, among other molecules, the analysis of Cu_3,[23] Na_3,[24] Ag_3,[25] and Li_3 [26] spectra. These studies demonstrate that even for moderate values of the distortion parameter k, one expects an extended progression in the e' mode for a transition between a Jahn–Teller distorted state and an undistorted D_{3h} state. This is exactly the situation for the Si_3 ($^3A_2'$) $\leftarrow Si_3^-$ transition in our ZEKE spectrum. The key question then is whether the smaller peak energies and intensities can be better explained assuming a Jahn–Teller distorted anion rather than a rigid, C_{2v} anion.

We first consider the anion energy levels. For k sufficiently large, the vibrational energy level patterns should approximately follow the familiar formula for a freely pseudorotating species[21]

$$E=\hbar\omega_1(\nu_1+\tfrac{1}{2})+\hbar\omega_2(\nu_2+\tfrac{1}{2})+Aj^2, \tag{2}$$

where ω_1 is the symmetric stretch frequency, ω_2 is as defined above, ν_1 and ν_2 are the quantum numbers associated with ω_1 and ω_2, and j is the half-integer pseudorotation quantum number. The pseudorotation constant A is inversely proportional to the reduced mass and the square of the equilibrium distortion along the e' coordinate ($\hbar/2\mu\rho_0^2$). This produces an energy level pattern similar to that shown in Fig. 4, where the anion levels are labeled (ν_1, ν_2, j). Deviations from the energy level pattern of Eq. (2) occur when k^2 is small (very small distortion), or when there is any barrier to pseudorotation.

In the limit of linear vibronic coupling [Eq. (1)], transitions from a particular j level of the anion are allowed to $l=j\pm 1/2$ levels in the neutral, where l is the vibrational angular momentum for the (D_{3h}) neutral species. The allowed neutral $\leftarrow$anion transitions [and the forbidden transition (peak a) which is discussed below] are indicated by arrows in Fig. 4. This figure suggests an alternate explanation for several of the lower intensity peaks in the ZEKE spectrum, namely, that they are "hot bands" originating from excited pseudorotational states of the anion, rather than from excited vibrational levels as assumed in the "rigid anion" Franck–Condon analysis. Thus, the sequence transitions between the 0,0,3/2 level and the neutral $\nu_2\geq 1$ levels would account for peaks 2′–4′, etc., while the transitions from the 0,0,5/2 level to the neutral $\nu_2\geq 2$ levels account for peaks a_1–a_3.

We can determine if this assignment is reasonable by computing the pseudorotation constant A in Eq. (2) from the energy difference between peaks 1 and 2′ in the experimental spectrum, assuming that these are the 0,1,1$\leftarrow$0,0,1/2 and the 0,1,1$\leftarrow$0,0,3/2 transitions, respectively. This difference is 80 cm^{-1}, yielding A=40 cm^{-1} and $\sqrt{\mu}\rho_0 = 0.11$ Å $amu^{1/2}$. The latter value is very similar

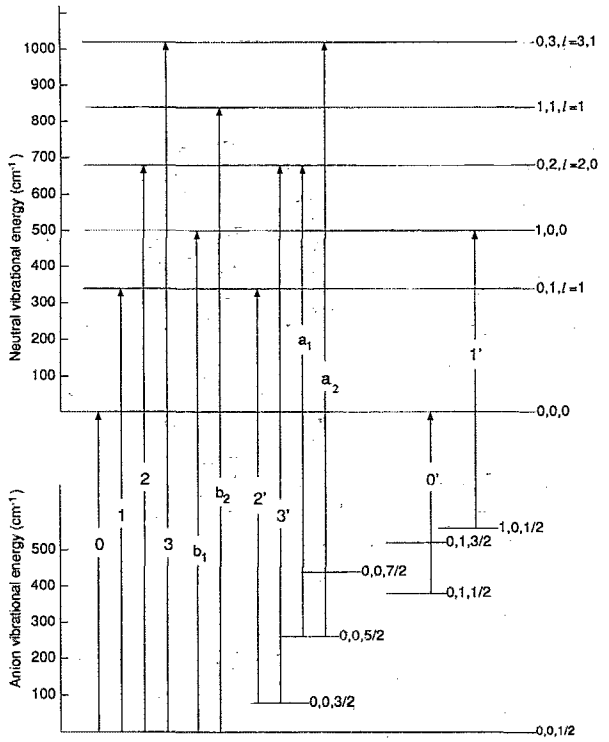

FIG. 4. A schematic of Si_3 and Si_3^- energy levels and some of the transitions proposed in the spectral assignment (see Table I for the complete assignment).

to the 0.095 Å amu$^{1/2}$ normal coordinate displacement determined from the Franck–Condon simulation as well as the *ab initio* displacement, indicating that our value for A is certainly acceptable. However, with such a small distortion, Eq. (2) may not give a good approximation of the actual energy levels.

To proceed further, we need to simulate the ZEKE spectrum including the effects of Jahn–Teller coupling in the anion. This requires that we solve Eq. (1) for the anion wave functions and energy levels, varying k to best match the intensity pattern of the main bending progression. The energy levels are obtained in terms of ω_2, the (undistorted) harmonic e' frequency, which can then be extracted by scaling the simulated spectrum to match the spacing between peaks 0 and 0′. Intensities are determined by calculating the overlap between the anion and neutral nuclear wave functions; as before, the symmetric stretch mode is assumed to be uncoupled to the e' mode. The anion bend eigenfunctions of Eq. (1) are linear combinations of harmonic oscillator wave functions with frequency ω_2 and, for the purpose of intensity calculations only, the neutral e' wave functions are taken to be harmonic with frequency ω_2. As long as the neutral e' frequency of 337 cm^{-1} differs only sightly from ω_2 [which it does (see below)] this approximation will have a negligible effect on the calculated intensities. Transitions from levels as high as the (1,0,3/2) level ($\sim$650 cm^{-1}) were considered in these simulations.

The best simulation, shown in the third panel of Fig. 3, was obtained with $k=1.9$. As expected, such a small k gives vibrational and pseudorotational energy levels deviating sightly from Eq. (2). For instance, the separation of the first two $j=1/2$ levels is $\sim 1.1\ \omega_2$ [as opposed to ω_2 per Eq. (2)] which should equal the 385 cm^{-1} frequency determined from hot band 0′. From this, we find $\omega_2=350$ cm^{-1}, which, as would be expected, falls between the calculated a_1 (297 cm^{-1}) and b_2 (370 cm^{-1}) frequencies for the distorted $^2A_1$ state.[17] Moreover, the energies of the $j=5/2$ and $j=3/2$ levels with respect to the ground $j=1/2$ level are not at a ratio of 3:1, as given by Eq. (2).

The overall agreement with the experimental spectrum is reasonable, supporting the assignments discussed above. One nice feature is that the peak marked with the ☆ in the rigid anion simulation is absent, in better agreement with the experiment; this peak would correspond to the $(0,1,1)\leftarrow(0,0,5/2)$ transition, which is forbidden by the $l=j\pm 1/2$ selection rule. However, the linear Jahn–Teller simulation still has some shortcomings. The energy separation between the two lowest levels of the anion—the (0,0,1/2) and (0,0,3/2) levels—is 0.311 ω_2 (110 cm^{-1}). Consequently, transitions originating from the (0,0,3/2) level, marked with circles in the simulation, are slightly to the red of the experimental sequence bands (peaks 2′–4′). This small overestimation of the $j=3/2$ level has also been seen in other calculations for several of the excited states of Na_3.[27] As with the rigid anion simulation, $\Delta v_1=0$ sequence bands from the 1,0,1/2 anion level fall approximately 50–60 cm^{-1} to the red of the main progression members, so there are two peaks to the red of each of the main peaks 1–3, as opposed to one in the experimental spectrum. Finally, the small peak a, found 280 cm^{-1} to the red of the origin, energetically appears to be the transition from the (0,0,5/2) level to the ground vibrational level of the neutral, but this transition is not allowed because of the (l,j) selection rule.

We can, however, attempt to better align the n' sequence bands both by increasing k slightly, which lowers the energy of the (0,0,3/2) level, and by including the quadratic coupling term $\frac{1}{2}g\rho^2e^{\pm 2i\phi}$ in Eq. (1). This results in a barrier to pseudorotation given by $E_{\rm loc}=gk^2\omega_0/(1-g^2)$,[21] which splits the degenerate $j=3/2$ levels substantially.[22] Additionally, this quadratic term couples the $j=1/2$ level with the $j=5/2$ level (through the ρ^2 term), resulting in nonzero intensity for the $(0,0,0)\leftarrow(0,0,5/2)$ transition believed responsible for peak a. The effects of these two modifications are shown in the bottom panel of Fig. 3. For this simulation, $k=2.0$ and $g=0.005$ in the quadratic coupling term. With these parameters, $E_{\rm loc}=7$ cm^{-1}, the (0,0,3/2) level is split by 20 cm^{-1} [the resulting levels are labeled (0,0,3/2±) in Table 1], and the stabilization energy is 725 cm^{-1}. We now observe only one resolved peak to the red of each of the peaks 1–3, and the placement agrees with the experimental peaks 2′–4′. The simulation shows several weak features which appear to correspond to peak a as well as some of the other peaks to the red of the origin.

We also attempted to adjust the linear and quadratic parameters to give a greater barrier to pseudorotation, as it has been calculated to be 160 cm^{-1}. However, the spec-

trum could not be simulated assuming such a high barrier. For instance, with $k=1.8$ and g determined using $E_{loc}=160\ cm^{-1}$, the simulated bend progression was far too extended. We also varied k and g to give a larger barrier and a shorter progression, but the sequence band structure obtained from these variations was in much worse agreement with the experimental sequence band structure.

While none of the three simulations shown in Fig. 3 exactly match the experimental spectrum (most notably, peak 1″ is still unassigned), the quadratic Jahn–Teller treatment is superior to the other two. The "rigid anion" treatment did not correctly match the experimental sequence band transitions, and the anion ν_2 and ν_3 frequencies determined from this analysis were the reverse of the calculated values. In the linear Jahn–Teller limit, several of the simulated sequence peaks were again mispositioned, but the overall profile of the spectrum was better matched. The quadratic Jahn–Teller coupling treatment yielded a closer overall match of the simulated and experimental peaks. Moreover, the quadratic model is consistent with the *ab initio* prediction of a small barrier to pseudorotation, although we find the barrier to be even lower than calculated. The peak assignments based on the quadratic Jahn–Teller simulations are given in Table I. Several of the peaks consist of overlapping transitions, and in these cases, the transitions are listed in order of descending contribution. Note that the composition of peaks 2′–4′ is quite different from peaks 0′ and 1′, even though they appear to be part of a single progression. Also note that there are no changes in the assignments of peaks n, b_n, and 0′ from the rigid anion analysis of Sec. III A, although the notation is somewhat different.

C. Role of the $^1A_1$ state

Figure 1 shows that the extent of the ZEKE spectrum is considerably less than that of band X in the PES. Moreover, the ZEKE intensity falls off dramatically just where band X degenerates into a mass of unresolved signal at lower electron kinetic energies. This congested signal in the PES is more likely due to transitions to the $^1A_1$ state of the neutral. From the calculated anion and neutral geometries and the form of the normal coordinates, we determine the normal mode displacement to be 0.043 and 0.314 Å $amu^{1/2}$ for the ν_1 and ν_2 modes, respectively. Displacement of this magnitude would produce a much longer progression in the ν_2 mode (in addition to significant activation in the ν_1 mode) than what is observed in the ZEKE spectrum of the X band.

As a first order approach to determine the extent to which the $^1A_1+e^-\leftarrow{}^2A_1$ transition contributes to the PES X band, we can simulate this transition at an arbitrary origin and then convolute it with the PES experimental resolution. We can then add it to the simulation of the $^3A_2'+e^-\leftarrow{}^2A_1$ transition, also convoluted with the PES resolution, adjusting the origin and the electronic transition moment of the $^1A_1$ simulation until the profile of the PES X band is matched. Figure 5 shows the result of the added simulations with the origin of the $^1A_1+e^-\leftarrow{}^2A_1$ transition placed 10 meV below the origin of the

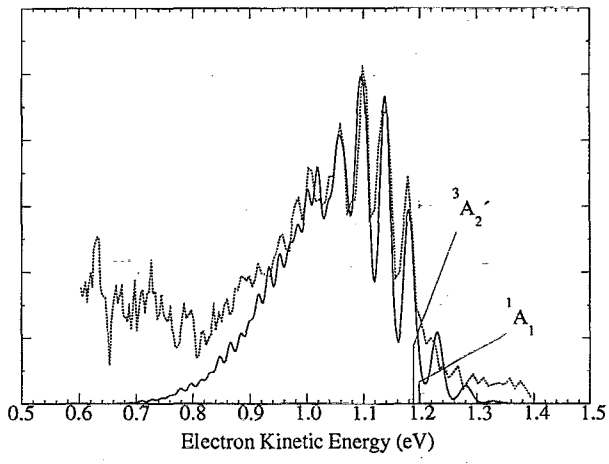

FIG. 5. Simulation of band X in the Si_3^- photoelectron spectrum including contributions from (a) the $^3A_2'+e^-\leftarrow{}^2A_1$ transition, in which the experimental ZEKE spectrum is convoluted with the lower resolution of the photoelectron spectrometer, and (b) the $^1A_1+e^-\leftarrow{}^2A_1$ transition, which was simulated using *ab initio* frequencies and geometries for the anion and neutral. Origins for the two bands are indicated with arrows; the origin for the singlet band is adjusted to best match the experiment.

$^3A_2'+e^-\leftarrow{}^2A_1$ transition. However, we hesitate to make any final comment as to the actual ground state based on this somewhat crude analysis.

It still remains that the transition to the $^1A_1$ state is not apparent in the ZEKE spectrum. This state is formed by removing the lone a_1 electron from the ion [refer to configuration (3)], while the $^3A_2'$ state is formed by removing a b_2 electron. Following the Wigner threshold law[28] and the selection rules developed by Reed *et al.*,[29] the total photodetachment cross sections near threshold for both of these states should be proportional to $\sigma_0\ (E_{h\nu}-E_{threshold})^{1/2}$, which rises sharply just above photodetachment threshold (s-wave detachment). However, it appears to be the case that σ_0 near threshold for the former transition is considerably smaller than for the latter. Interestingly, band B in the Si_3^- photoelectron spectrum, which was assigned to the $^3A_1+e^-\leftarrow{}^2A_1$ transition,[17] also involves the removal of a lower-lying a_1 electron. While band B is the most prominent feature in the PES, the cross section near threshold for this band was too small to obtain higher resolution ZEKE spectra.

V. CONCLUSIONS

The analysis of the extensive vibrational structure in the ZEKE spectrum of Si_3^- shows that the spectrum is due to the $^3A_2'+e^-\leftarrow{}^2A_1$ transition. Progressions in the bending and symmetric stretch modes of the neutral are observed, yielding frequencies of 337 and 501 cm^{-1}, respectively. A comparison of these frequencies with *ab initio* values shows that agreement is best with several of the density functional calculations. The ZEKE spectrum shows several smaller features in addition to the main progressions. These are best explained by treating the anion as a fluxional species with some pseudorotational excitation;

the smaller peaks are then assigned to sequence bands originating from these excited levels of the anion.

A comparison of the Si_3^- PES and ZEKE spectrum suggests that band X in the PES consists of overlapping transitions to the neutral $^1A_1$ and $^3A_2'$ states, but the transitions to the $^1A_1$ state do not appear in the ZEKE spectrum. This is presumably due to a small photodetachment cross section for the transition to the singlet state near the detachment threshold. Unfortunately, this means we cannot determine which state of Si_3 is the true ground state, although simulations of band X using *ab initio* geometries suggest that it is the singlet state.

Note added in proof. Honea *et al.*[30] have recently published Raman spectra of Si_4, Si_6, and Si_7. Hence, our statement in the opening paragraph needs amendment.

ACKNOWLEDGMENTS

This work was supported under NSF grant no. DMR-9201159. We would like to thank Michele Dupuis and Celeste McMichael Rohlfing for helpful conversations.

[1] P. W. Merril, Publ. Astron. Soc. Pac. **38**, 175 (1926); R. F. Sanford, Astrophys. J. **111**, 262 (1950); B. Kleman, *ibid.* **123**, 162 (1950) and references therein.
[2] P. Ho and W. G. Breiland, Appl. Phys. Lett. **44**, 51 (1984).
[3] R. O. Jones, Phys. Rev. A **32**, 2589 (1985); K. Raghavachari and V. Logovinsky, Phys. Rev. Lett. **55**, 26 (1985); G. Pacchioni and J. Koutecky, J. Chem. Phys. **84**, 3301 (1986); Z. Slanina, Chem. Phys. Lett. **131**, 420 (1986); D. Tomanek and M. A. Schluter, *ibid.* **56**, 1055 (1986); K. Balasubramanian, Chem. Phys. Lett. **135**, 283 (1987); K. Raghavachari, Z. Phys. D **12**, 61 (1989); C. M. Rohlfing and K. Raghavachari, Chem. Phys. Lett. **167**, 559 (1990); S. D. Li, R. L. Johnston, and J. N. Murrell, J. Chem. Soc. Faraday Trans. **88**, 1229 (1992).
[4] A. E. Douglas, Can. J. Phys. **33**, 801 (1955); R. D. Verma and P. A. Warsop, *ibid.* **41**, 152 (1963); I. Dubois and H. Leclerq, *ibid.* **49**, 3053 (1971); S. P. Davis and J. W. Brault, J. Opt. Soc. Am. B **4**, 20 (1987); M. R. Nimlos, L. B. Harding, and G. B. Ellison, J. Chem. Phys. **87**, 5116 (1987).
[5] T. N. Kitsopoulos, C. J. Chick, Y. Zhao, and D. M. Neumark, J. Chem. Phys. **95**, 1441 (1991); C. C. Arnold, T. N. Kitsopoulos, and D. M. Neumark, *ibid.* **99**, 766 (1993).
[6] T. N. Kitsopoulos, C. J. Chick, A. Weaver, and D. M. Neumark, J. Chem. Phys. **93**, 6108 (1990).
[7] C. B. Winstead, K. X. He, D. Grantier, T. Hammond, and J. L. Gole, Chem. Phys. Lett. **181**, 222 (1991).
[8] C. C. Arnold and D. M. Neumark, J. Chem. Phys. **99**, 3353 (1993).
[9] R. S. Grev and H. F. Schaefer, Chem. Phys. Lett. **119**, 111 (1985).
[10] K. Raghavchari, J. Chem. Phys. **83**, 3520 (1985).
[11] L. Gausset, G. Herzberg, A. Lagerqvist, and B. Rosen, Discuss. Faraday Soc. **35**, 113 (1963); Astrophys. J **142**, 45 (1967).
[12] D. A. Dixon and J. L. Gole, Chem. Phys. Lett. **188**, 560 (1992).
[13] M. Dupuis (private communication).
[14] R. Fournier, S. B. Sinnott, and A. DePristo, J. Chem. Phys. **97**, 4149 (1992).
[15] J. R. Sabin, J. Oddershede, G. H. F. Diercksen, and N. E. Gruner, J. Chem. Phys. **84**, 354 (1986); K. Raghavachari *ibid.* **84**, 5672 (1986); K. Balasubramanian Chem. Phys. Lett. **125**, 400 (1986).
[16] K. Raghavachari and C. M. Rohlfing, J. Chem. Phys. **94**, 3670 (1991).
[17] C. M. Rohlfing and K. Raghavachari, J. Chem. Phys. **96**, 2114 (1992).
[18] O. Cheshnovsky, S. H. Yang, C. L. Pettiette, M. J. Craycraft, Y. Liu, and R. E. Smalley, Chem. Phys. Lett. **138**, 119 (1987).
[19] T. N. Kitsopoulos, I. M. Waller, J. G. Loeser, and D. M. Neumark, Chem. Phys. Lett. **159**, 300 (1989); C. C. Arnold, Y. Zhao, T. N. Kitsopoulos, and D. M. Neumark, J. Chem. Phys. **97**, 6121 (1992).
[20] K. Müller-Dethlefs, M. Sander, and E. W. Schlag, Z. Naturforsch Teil A **39**, 1089 (1984); Chem. Phys. Lett. **12**, 291 (1984); K. Müller-Dethlefs and E. W. Schlag, Annu. Rev. Phys. Chem. **42**, 109 (1991).
[21] H. C. Longuet-Higgens, U. Opik. M. H. L. Price, and R. A. Sack, Proc. R. Soc. London Ser. A **244**, 1 (1958); H. C. Longuet-Higgens, Adv. Spectrosc. **2**, 429 (1961).
[22] R. L. Whetten, G. S. Ezra, and E. R. Grant, Annu. Rev. Phys. Chem. **36**, 277 (1985); R. L. Whetter, K. S. Haber, and E. R. Grant, J. Chem. Phys. **84**, 1271 (1985).
[23] M. D. Morse, Chem. Phys. Lett. **133**, 8 (1987); E. A. Rohlfing and J. J. Valentini, *ibid.* **126**, 113 (1986); M. D. Morse, J. B. Hopkins, P. R. R. Langridge-Smith and R. E. Smalley, J. Chem. Phys. **79**, 5316 (1983); M. Moskovits, Chem. Phys. Lett. **118**, 111 (1985).
[24] G. Delacrétaz, E. R. Grand, R. L. Whetten, L. Wöste, and J. Zwanziger, Phys. Rev. Lett. **56**, 2598 (1986).
[25] K. Laitting, P. Y. Cheng, and M. A. Duncan, Chem. Phys. Lett. **152**, 341 (1988); P. Y. Cheng and M. A. Duncan, *ibid.* **156**, 420 (1989); A. M. Ellis, E. S. J. Robles, and T. A. Miller, *ibid.* **201**, 132 (1993).
[26] Ph. Dugourd, J. Chevaleyre, M. Broyer, J. P. Wolf, and L. Wöste, Chem. Phys. Lett. **175**, 555 (1990).
[27] G. Delecrétaz, E. Grant, R. L. Whetten, L. Wöste, and J. Zwanziger, Phys. Rev. Lett. **56**, 2598 (1986); M. Bröyer, G. Delecrétaz, G.-L. Ni, R. L. Whetten, J. P. Wolf, and L. Wöste, J. Chem. Phys. **90**, 843 (1989).
[28] E. P. Wigner, Phys. Rev. **73**, 1003 (1948).
[29] K. J. Reed, A. H. Zimmerman, H. C. Andersen, and J. I. Brauman, J. Chem. Phys. **64**, 1368 (1976).
[30] E. C. Honea, A. Ogurn, C. A. Murray, K. Raghavachari, W. D. Sprenger, M. F. Jarrold, and W. L. Brown, Nature **366**, 42 (1993).